Two-Dimensional Short-Range Magnetic Order in the Tetragonal Spinel $Li_2Mn_2O_4$

A. S. Wills,† N. P. Raju, C. Morin, and J. E. Greedan*

Brockhouse Institute for Materials Research, McMaster University, 1280 Main Street West, Hamilton, Ontario, Canada, L8S 4M1

Received March 24, 1999. Revised Manuscript Received May 17, 1999

Metastable, tetragonal $Li_2Mn_2O_4$, prepared by chemical insertion of Li into the cubic spinel, $LiMn_2O_4$, was studied by dc magnetic susceptibility and neutron diffraction. The susceptibility data show a very broad maximum at about 120 K, a sharp maximum at about 50 K, and no evidence for Curie−Weiss behavior even up to 600 K. This is consistent with the dominance of short-range, antiferromagnetic correlations attributed to the geometrical frustration inherent in the Mn^{3+} sublattice which is a slightly distorted pyrochlore lattice, a three-dimensional array of corner-sharing tetrahedra. The temperature dependence of two diffuse peaks in the neutron diffraction data correlate well with the 50 K anomaly but show, remarkably, an asymmetric Warren line-shape characteristic of two-dimensional correlations with no sign of long-range order down to 1.6 K. The magnetic reflections can be indexed as (2 0) and (1 3) of a $\sqrt{3} \times \sqrt{3}$ magnetic structure arising from a Kagomé layer. The structure and properties of tetragonal $Li_2Mn_2O_4$ are compared with the thermodynamically stable orthorhombic form.

1. Introduction

The lithium manganate series $Li_xMn_2O_4$, where $x = 0-2$, has been extensively investigated electrochemically due to a potential use as cathode materials in secondary lithium ion batteries. The principal reaction is the reversible insertion and deinsertion of lithium into and from the $LiMn_2O_4$ host. If such insertion and deinsertion is stoichiometric, tetragonal $Li_2Mn_2O_4$ and λ-MnO_2 are formed, respectively. Investigation into the mechanism for the insertion of the second lithium at 3 V is complicated by phase separation and possible redistribution of Li^+ ions between octahedral (8c) and tetrahedral (4a) sites, and so is still a matter for conjecture. The presence of the Jahn−Teller active Mn^{3+} species in t-$Li_2Mn_2O_4$ and an average Mn valency v(Mn) < 3.5 leads to a tetragonal distortion away from the cubic spinel structure and a corresponding drop in the open circuit voltage from ∼4 V for $0 \leq x \leq 1$, to ∼3 V for $1 \leq x \leq 2$. The crystal structure of t-$Li_2Mn_2O_4$ has the tetragonal $[Mn^{3+}{}_2]O_4$ framework of the spinel hausmannite $Mn^{2+}[Mn^{3+}{}_2]O_4$ and is described in the $I4_1/amd$ space group. In contrast with the closely related systems $Li_2V_2O_4$ and $Li_2Ti_2O_4$, where the Li^+ ions occupy all the available octahedral sites, David et al.[1] suggested that in t-$Li_2Mn_2O_4$ the repulsions between Mn^{3+} (8d)−Li^+ (8c) interactions are sufficiently strong to force some of the Li ions onto the 4a sites.[2]

For compositions in the range, $1 \leq x \leq 2$, the $Li_xMn_2O_4$ is found to phase separate into tetragonal $Li_2Mn_2O_4$ and cubic $LiMn_2O_4$.[2,3] Calculations have shown that the drastic change in the open circuit voltage at $x = 1$ is due to a combination of both the valency change of the Mn ions during the phase separation and the occupation of the 16c sites, but is not a simple result of repulsions between the ions on the 8d and 8c sites.[3] Insertion of lithium beyond $x = 2$ leads to a further distortion to the hexagonal $Li_{2-y}MnO_2$ structure.[4]

In addition to the importance of the $Li_xMn_2O_4$ system in current electrochemistry, the basic structure and electronic properties, such as electrical transport and magnetism, of several members are also attracting attention. For example the metastable phases, cubic λ-MnO_2 and tetragonal $Li_2Mn_2O_4$, obtainable by ambient temperature chemical (as well as electrochemical) Li insertion or deinsertion of the cubic spinel, $LiMn_2O_4$, retain the basic spinel structure and thus present different geometries than β-MnO_2 and orthorhombic $LiMnO_2$, the respective thermodynamically stable forms. In terms of their magnetism, these spinel phases behave quite differently: λ-MnO_2 exhibits a very complex antiferromagnetic ordering[5] for example and $LiMn_2O_4$ undergoes a charge ordering, first-order structural phase transition below 280 K and also very complex magnetic ordering at low temperatures.[6] In this work the magnetic properties of tetragonal $Li_2Mn_2O_4$ are investigated. In the spinel structure the topology of the Mn sublattice is a three-dimensional network of corner-sharing tetrahedra, the so-called pyrochlore lattice of vertex-sharing tetrahedra (Figure 1). Antiferromagnets

† Current address: Centre D'Études Nucléaires de Grenoble, DRFMC/SPSMS/MDN, 17 Rue des Martyrs, 38054 Grenoble, Cédex 9, France.

(1) David, W. I. F.; Thackeray, M. M.; de Picciotto, L. A.; Goodenough, J. B. *J. Solid State Chem.* **1987**, *67*, 316.

(2) Thackeray, M. M.; David, W. I. F.; Bruce, P. G.; Goodenough, J. B. *Mater. Res. Bull.* **1983**, *18*, 461.

(3) Miura, K.; Yamada, A.; Tanaka, M. *Electrochim. Acta* **1996**, *41*, 249.

(4) David, W. I. F.; Goodenough, J. B.; Thackeray, M. M.; Thomas, M. G. S. R. *Rev. Chim. Minér.* **1983**, *20*, 636.

(5) Greedan, J. E.; Raju, N. P.; Wills, A. S.; Morin, C.; Shaw, S. M.; Reimers, J. N. *Chem. Mater.* **1998**, *10*, 3058.

(6) Wills, A. S.; Raju, N. P.; Greedan, J. E. *Chem. Mater.* **1999**, *11*, 1510.

10.1021/cm990175b CCC: $18.00
Published on Web 07/01/1999

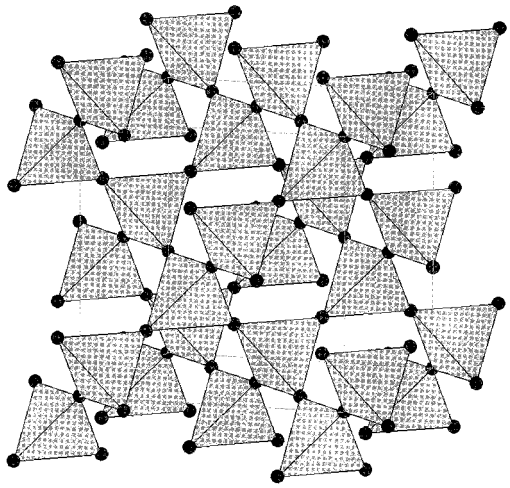

Figure 1. The pyrochlore lattice made up of vertex-sharing tetrahedra.

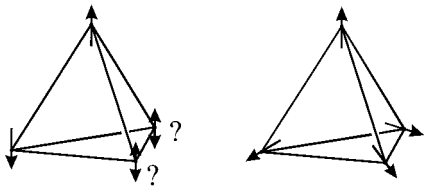

Figure 2. (a) A frustrated arrangement of spins on a tetrahedron and (b) the compromise arrangement of canted moments at 109° to each other.

which have this connectivity are described as being frustrated[7,8] because four moments at the vertexes of a tetrahedron cannot align themselves in such a way as to be simultaneously antiparallel to each other (Figure 2a), and the tendency for neighboring moments to align antiferromagnetically causes them to adopt a canted configuration in which the vector sum of the moments over a tetrahedron is 0 (Figure 2b). In addition to being frustrated, the pyrochlore lattice is of special interest because the connectivity of the tetrahedra is such that the criterion of the vector sum of moments on each tetrahedron being 0 is insufficient to define an unique spin structure. This results in the system having a large number of degenerate lowest-energy spin configurations and correspondingly, a difficulty in the selection of an unique ground state.[9] Indeed, experimental realizations have been found to possess a highly degenerate ground-state manifold.[10] Particular ground states may be selected from within this manifold by the introduction of further-neighbor interactions.[11] Which structure is chosen depends on the relative strengths of the further-neighbor exchange pathways. In the cubic spinels the geometry of the crystal structure allows further-neighbor interactions that are of comparable strength to those of the nearest-neighbors. These can result in the formation of highly complex magnetic structures that cannot be explained solely on the basis of further neighbor exchange, as observed in λ-MnO_2 and $LiMn_2O_4$.

2. Experimental Section

2.1. Preparation. $Li_2Mn_2O_4$ was prepared by lithiation of $LiMn_2O_4$ using ^{n}Bu−Li. $LiMn_2O_4$ was synthesized from Li_2CO_3 (J.T. Baker Chemical Co., 99.1%) and Mn_2O_3 (Alfa Inorganics, Ventron, 98%). Stoichiometric quantities were thoroughly ground under acetone, and the dried mixture was pelletized. The pellets were prefired in air at 650 °C for 12 h before being heated to 800 °C. They were held at this temperature for 24 h and then cooled to room temperature. To improve homogeneity the product was ground, repelletized, and again fired at 800 °C. Three grams of the resulting $LiMn_2O_4$ was then reacted at room temperature under an argon atmosphere with 12.5 mL of 16 M ^{n}Bu−Li in 40 mL of sodium-dried hexane.[2,12]This ratio provides ∼20% excess ^{n}Bu−Li. An immediate color change of the suspension from black to brown was observed, and the reaction was left to proceed for 5 days at 50 °C with constant stirring. The product was then filtered under reduced pressure and washed several times with sodium-dried hexane before being dried under vacuum. Any remaining ^{n}Bu−Li is highly air-sensitive, so care was taken to wash the slurry thoroughly and all subsequent handling was carried out in an inert atmosphere. The resulting t-$Li_2Mn_2O_4$ was found to be phase pure by XRD.

2.2. Direct Current Susceptibility. Direct current (dc) susceptibility measurements were taken using a Quantum Design MPMS SQUID magnetometer between 2 and 600 K. Data were taken with the sample held in a sealed quartz tube and cooled in a measuring field of 100 Oe. Corrections were made for the diamagnetic contribution of the constituent ions.

2.2. Neutron Diffraction. The crystal structure was verified using neutron diffraction data collected at 20 K from a sample held in an aluminum can at the McMaster reactor with neutrons of wavelength 1.392 Å. Low-angle data are contaminated by magnetic scattering and so data up to 28° were excluded from the refinement. Analysis of the magnetic structure was performed using neutron diffraction data collected with the high-resolution C2 diffractometer of the DUALSPEC facility at AECL, Chalk River Laboratories. Diffraction patterns from a sample held in a vanadium can were collected with neutrons of wavelength 2.3713 Å, between 1.6 and 150 K out to a momentum transfer of $\mathbf{q} = 3.51$ Å^{-1}. Rietveld refinement was carried out using version 6 of the PC translation of the GSAS suite[13] and bond-valence calculations with the program VaList.[14]

3. Results

The crystal structure of t-$Li_2Mn_2O_4$ is described in space group $I4_1/amd$.[2] Mn atoms reside in octahedrally coordinated 8d sites and oxygen on 16h sites (Figure 3). Previous neutron diffraction studies indicated that in t-$Li_2Mn_2O_4$ the Li atoms are statistically distributed over both octahedral 8c sites and tetrahedral 4a sites.[1] However, the low resolution of the dataset and overlap with the aluminum sample can peaks obscured the weak reflections that signal occupation of the 4a sites.[1] In the refinement, the presence of Li on the 4a sites did not improve the quality of the fit and so final cycles were carried out with only occupation of the 8c sites. The refined profile is shown in Figure 4, the refinement details are presented in Table 1 and selected interatomic distances and angles are collected in Table 2 along with corresponding entries for o-$LiMnO_2$.[15] Overlap of aluminum peaks with those of the spinel at 41° and 58° combined with an inability to model the preferred

(7) Anderson, P. W. *Phys. Rev.* **1956**, *102*, 1008.
(8) Villain, J. *Z. Phys. B* **1979**, *33*, 31.
(9) Reimers, J. N. *Phys. Rev. B Condens. Matter* **1992**, *45*, 7287.
(10) Reimers, J. N.; Greedan, J. E.; Kremer, R. K.; Gmelin, E.; Subramanian, M. A. *Phys. Rev. B Condens. Matter* **1991**, *43*, 3387.
(11) Reimers, J. N.; Berlinsky, A. J.; Shi, A. C. *Phys. Rev. B Condens. Matter* **1991**, *43*, 865.
(12) Whittimgham, M. S.; Dines, M. B. *J. Electrochem. Soc.* **1977**, *124*, 1387.
(13) Larsen, A. C.; von Dreele, R. B. *GSAS General Structure Analysis System*; University of California: San Marcos, 1994.
(14) Wills, A. S.; Brown, I. D. *VaList*; CEA: France 1999. Program available from author at willsas@netscape.net.

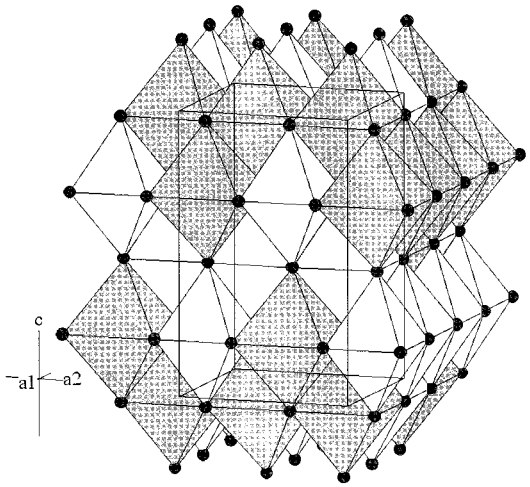

Figure 3. Polyhedral representation of the tetragonal structure of $Li_2Mn_2O_4$. The Mn octahedra are darker.

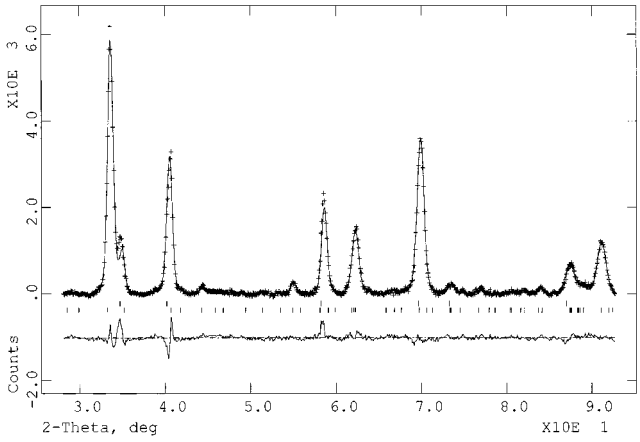

Figure 4. Fit of the refined profile to the neutron powder diffraction pattern of t-$Li_2Mn_2O_4$ taken at 20 K with neutrons of wavelength 1.3920 Å.

orientation and axial stress that result from the rolling process used in the production of the aluminum cans, lead to the poor fit to the data at 41° and 58°. A very close correspondence exists between the nearest-neighbor (nn) and next-nearest-neighbor (nnn) bond distances and angles between the two structures. This is to be expected as both materials involve edge-sharing octahedra as the basic structural motif. The principal difference between the two structures is in the topology of the Mn sublattice. In the orthorhombic form this consists of stacks of puckered sheets and is distinctly two-dimensional (Figure 5) while in the tetragonal form, as pointed out earlier, one finds a three-dimensional array of corner-sharing tetrahedra.

Bond-valence analysis calculations were performed with the formula:

$$\sum_{ij} S_{ij} = \sum_{ij} \exp[(R_0 - R_{ij})/B] \qquad (1)$$

where, R_{ij} is the bond length and R_0 a distance characterizing the cation−anion bond, R_0 (Mn^{3+}−O^{2-}) = 1.760 and B is a "universal" constant equal to 0.37. The sum is over the bonded atoms i and j, and was carried out for the Mn(8d) site with the assumption of the manganese being successively in the third and fourth oxidation states. This gives bond-valence sums of 3.12 and 3.06, respectively, consistent with expectations.

The dc susceptibility as a function of temperature shows a broad maximum at ∼120 K and below that a sharp maximum (Figure 6). The derivative d(χT)/dT shows that T_c = 50 K. Examination of the inverse susceptibility−temperature plot shows the absence of any clearly linear regime up to 600 K. The same behavior was noted for orthorhombic $LiMnO_2$ where a Curie−Weiss range was found only between 600 and 800 K. This is not surprising as the nn and nnn Mn−O geometry, see Table 2, is essentially the same for both materials. For o-$LiMnO_2$ the $\theta_w = -1056$ K, indicating very strong antiferromagnetic interactions. Similarly large, negative values would be expected for t-$Li_2Mn_2O_4$.

$$\chi = \frac{C}{T - \theta_w} \qquad (2)$$

Deviations from Curie−Weiss linearity at temperatures that are high with respect to T_c is common in frustrated antiferromagnets and indicates that while the correlations are building up as the system is cooled, the frustration acts to hinder the formation of a Néel ordered state. A simple definition of a "frustration index", f, is given by[16]

$$f = \frac{|\theta_w|}{T_c} \qquad (3)$$

However, care must be taken in the use of f as a sole criterion for frustration as it is influenced greatly by further neighbor interactions and dimensionality. In t-$Li_2Mn_2O_4$ one can estimate a range of f between 12 and 20 which indicates that the system is indeed highly frustrated.

Neutron diffraction data (Figure 7) clearly show the presence of two broad temperature-dependent peaks at q = 1.22 and 2.00 Å^{-1}. Their temperature dependence, and the absence of any nuclear Bragg reflections in this region, indicate that they are due to magnetic scattering. The form of these broad asymmetric peaks: a sharp rise at low q and a slow fall off toward high q is characteristic of two-dimensional short-range order. The scattering from such a system is described analytically by a Warren function.[17] This function was originally developed to describe diffuse scattering of X-rays from forms of graphite, in which there is long-range structural order within a set of planes, but no structural correlations between these planes. It can be adapted to describe the diffuse magnetic scattering from a layered magnet in which there are long-range correlations within a plane, but no correlation between them, by the addition of a magnetic form factor $J(z)$. The static structure factor, $P_{2\theta}$, around the peak is then be expressed by

$$P_{2\theta} = Km \frac{{F_{hk}}^2(1 + \cos^2 2\theta)}{2(\sin\theta)^{3/2}} \left(\frac{L}{\lambda\sqrt{\pi}}\right)^{1/2} F(a)\cdot[J(z)]^2 \qquad (4)$$

(15) Hoppe, R.; Brachtel, G.; Jansen, M. *Z. Anorg. Allg. Chem.* **1975**, *1−10*, 417.
(16) Ramirez, A. P. *Annu. Rev. Mater. Sci.* **1994**, *24*, 453.
(17) Warren, B. E. *Phys. Rev.* **1941**, *59*, 693.

Table 1. Structural Parameters for t-$Li_2Mn_2O_4$ at 20 K in Space Group $I4_1/amd$ with $Z = 4$[a]

atom	*x*	*y*	*z*	frac	U_{iso}, Å^2	$\sum_{ij} S_{ij}$	site symmetry	Wyckoff site and multiplicity
Li1	0.0	0.7500	0.125	0			$-4m2$	4a
Li2	0.0	0.0	0.0	1	0.011 (8)	0.96	2/*m*	8c
Mn	0.0	0.0	0.5	1	0.008(4)	3.12	2/*m*	8d
O	0.0	0.4776(15)	0.2493(10)	1	0.0075 (15)	2.33	*m*	16h

[a] Cell parameters: $a = b = 5.6488$ (31) and $c = 9.198(5)$. $\chi^2 = 4.54$. $R_{wp} = 7.31\%$ for 26 variables. Total number of profile points = 647.

Table 2. Comparison of Relevant Distances and Angles for o-$LiMnO_2$ and t-$Li_2Mn_2O_4$

	o-$LiMnO_2$	t-$LiMnO_2$
Mn−O (Å)	2 × 1.895(4)	4 × 1.910(6)
	2 × 1.9554(4)	2 × 2.309(9)
	2 × 2.294(1)	
Mn−Mn (Å)	2 × 2.805(2)	2 × 2.842(2)
	4 × 3.098(2)	4 × 3.046(1)
Mn−O−Mn	93.3(1)	95.4(3)
(deg)	91.7(3)	91.9(3)
	170.6(3)	180
<Mn−O> (Å)	2.05	2.04

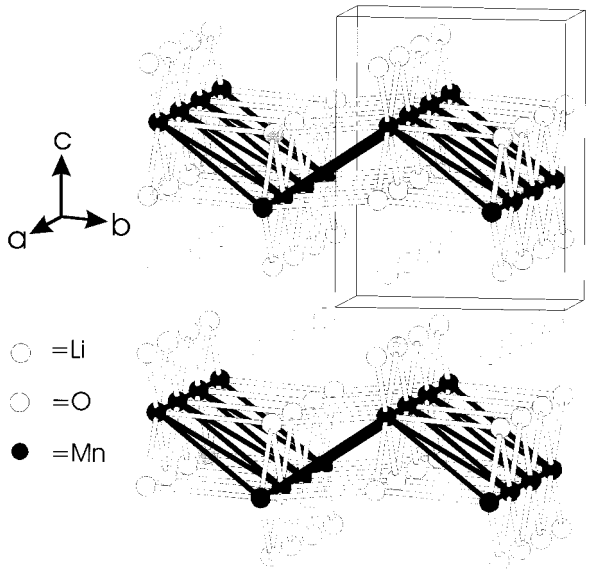

Figure 5. The crystal structure of o-$LiMnO_2$ with the distorted octahedral coordination of Mn and the Mn sublattice highlighted.

where

$$a = (2\sqrt{\pi}L/\lambda)(\sin\theta - \sin\theta_0) \quad (5)$$

and

$$F(a) = \int_0^{10} \exp[-(x^2 - a)^2]\, dx \quad (6)$$

L is the spin−spin correlation length, λ is the wavelength, K is a scaling constant, m is the multiplicity of the reflection, F_{hk} is the two-dimensional structure factor for the spin array, and θ_0 is the center of the peak. An error in the original paper was found: the integral for *F(a)* does not converge and for this work the calculation was performed using a finite integral; however, this does not lead to an appreciable difference in the results as the values for *F(a)* are the same as those tabulated in the original work of Warren. An example of such a fit to the data collected at 1.6 K is given in Figure 8 and the temperature dependence of the peak

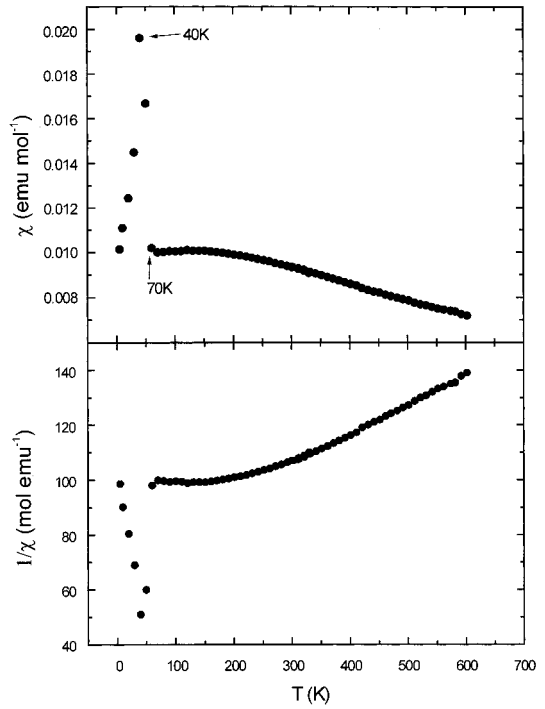

Figure 6. Zero-field-cooled dc susceptibility and inverse susceptibility for t-$Li_2Mn_2O_4$ as a function of temperature.

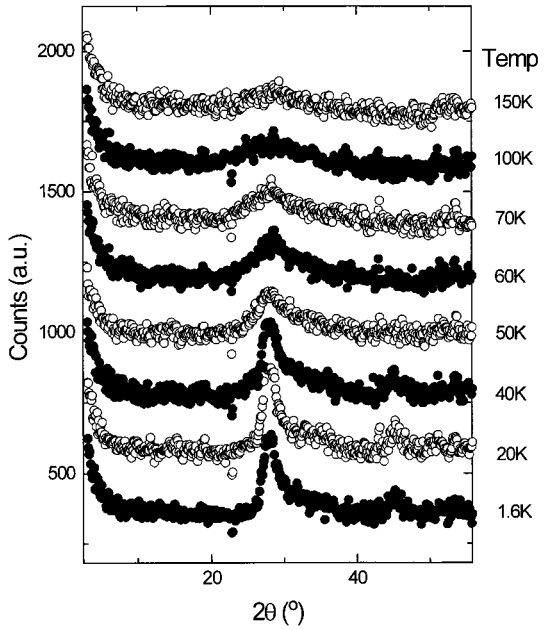

Figure 7. Powder neutron diffraction patterns of t-$Li_2Mn_2O_4$ taken between 1.6 K and 150 K with neutrons of wavelength 2.3713 Å.

is shown in Figure 7. The temperature dependence of the two-dimensional spin−spin correlation length from fits of eq 4 to the peak at $q = 1.22$ Å^{-1} is shown in Figure

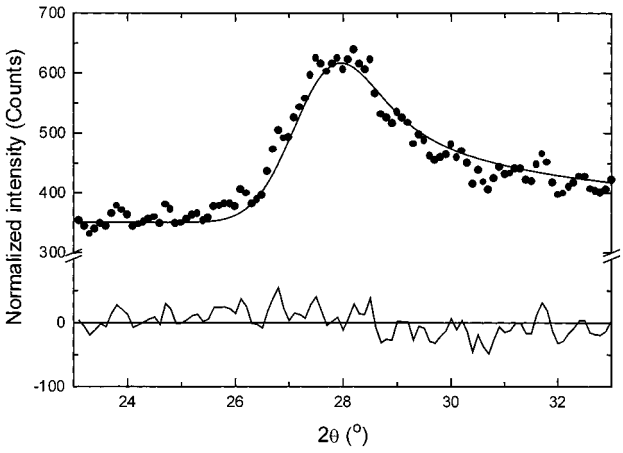

Figure 8. Fit of diffuse scattering of t-$Li_2Mn_2O_4$ at $q = 0.24$ Å^{-1} and 1.6 K to the Warren function.

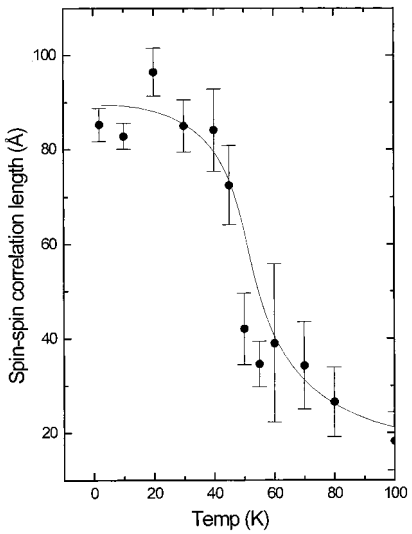

Figure 9. Static spin−spin correlation length determined from Warren function at $q = 0.24$ Å^{-1} as a function of temperature for t-$Li_2Mn_2O_4$ taken with neutrons of wavelength 2.3713 Å.

9. While the intensity of the second diffuse peak is far weaker than that of the first, within error the values of the fitted correlation lengths follow the same temperature dependence, and it appears that the transition observed in the dc susceptibility at 50 K is correlated with a change in the correlation length and is not due to the onset of any long-range ordered phase. The diffuse reflections also persist up to at least 150 K which corresponds to temperatures above the susceptibility maximum.

4. Discussion

While a transition to a short-range ordered system is not unexpected for a geometrically frustrated system, what is strange in this material is that the transition is apparently to a two-dimensional system of moments, given the three-dimensional nature of the superexchange pathways in the pyrochlore sublattice. Even with the inclusion of a tetragonal distortion away from the cubic spinel structure, the nearest-neighbor exchange system is still expected to be well-represented by the pyrochlore lattice. Examinations were carried out of various orbital ordering models, but a consequence of the crystal symmetry is that this cannot result in a two-dimensional exchange system. Therefore, the reason for the observed two-dimensionality must be due to some other property of the magnetic lattice, and the obvious starting place is to examine the pyrochlore structure in terms of possible two-dimensional planes.

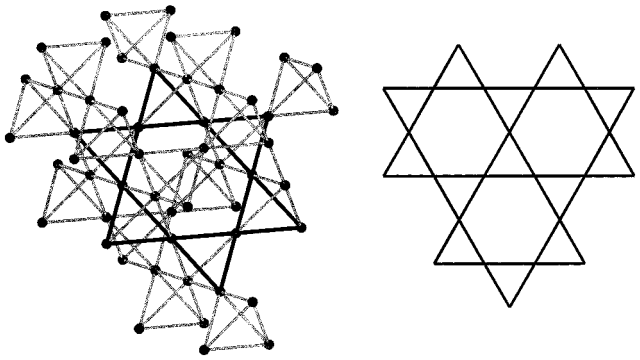

Figure 10. Planes taken perpendicular to body diagonal of the pyrochlore structure have the Kagomé structure.

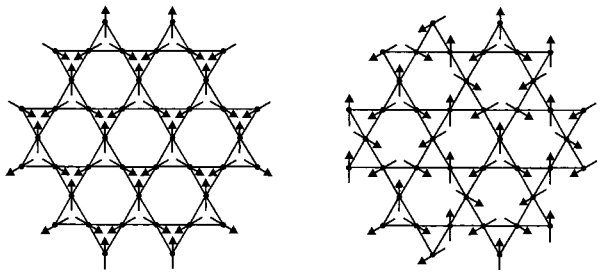

Figure 11. (a) $q = 0$ and (b) $\sqrt{3} \times \sqrt{3}$ spin configurations on the Kagomé lattice.

The most obvious planes are perpendicular to the body axes of the crystallographic cell, e.g., that corresponding to the (1 1 1) crystallographic plane. These planes present a Kagomé sublattice (Figure 10). The Kagomé lattice is of special significance as it is the two-dimensional analogue of the pyrochlore lattice, and they share many similar properties. For example, both are constructed of triangular plaquettes which share only one vertex with each neighboring triangle or tetrahedron and this topology leads to a highly degenerate ground state manifold that is not seen in other, more conventional lattice geometries. Because of this special connectivity both Kagomé and pyrochlore antiferromagnets are predicted to have large quantum fluctuations that act to destabilize a conventional Néel ordered ground state. Indeed, spin fluids and other non-Néel ground states have been predicted to exist in nearest-neighbor $S = {}^1/_2$ Kagomé and pyrochlore antiferromagnets.[9,11,18] The introduction of further-neighbor exchange has the effect of selecting particular highly symmetric ground states from the degenerate manifold. In the case of the Kagomé antiferromagnet spin wave theory shows that two particular spin configurations, termed the $q = 0$ and the $\sqrt{3} \times \sqrt{3}$ configurations (Figure 11), are believed to occur when $J_2 > J_3$ and when $J_2 < J_3$, respectively.[19] Taking the view of the Mn sublattice of the t-$Li_2Mn_2O_4$ structure as a system of Kagomé layers, it is interesting to examine the reflections that would

(18) Elser, V. *Phys. Rev. Lett.* **1989**, *62*, 2405.
(19) Harris, A. B.; Kallin, C.; Berlinsky, A. *J. Phys. Rev. B Condens. Matter* **1992**, *45*, 2899.

arise from either the $q = 0$ or the $\sqrt{3} \times \sqrt{3}$ spin structures. The in-plane lattice parameters of the distorted Kagomé net are $a = 6.092$ and $b = 5.649$ Å, and we find that the diffuse peaks are not compatible with the $q = 0$ spin structure but are compatible with the (2 0) and (1 3) reflections of the $\sqrt{3} \times \sqrt{3}$ spin structure.

5. Summary

The magnetic behavior of t-$Li_2Mn_2O_4$ has been investigated by both dc susceptibility and neutron diffraction. The susceptibility data are dominated by short-range order effects up to 600 K, resembling strongly the case of o-$LiMnO_2$ which has a layered structure. Not surprisingly, o-$LiMnO_2$ exhibits two-dimensional short-range order at high temperatures but a crossover to three-dimensional long-range order occurs below 261 K. o-$LiMnO_2$ is thus a fairly typical low dimensional magnet. In contrast, t-$Li_2Mn_2O_4$ retains the spinel structure, the Mn sublattice of which is a slightly distorted, three-dimensional pyrochlore network well-known to give rise to geometrical frustration and thus also consistent with an extensive short-range ordered regime as found in the susceptibility. The neutron diffraction data show that a prominent susceptibility anomaly at 50 K is not due to long-range order, but instead, remarkably, to a build up of two-dimensional spin−spin correlations which attain a maximum length of 80 Å. No sign of long-range order exists even at 1.6 K. This is inferred from the highly asymmetric shape of the diffuse magnetic scattering which can be fitted to a Warren function. Furthermore, the two prominent Warren features can be indexed as (2 0) and (1 3) reflections arising from a $\sqrt{3} \times \sqrt{3}$ spin arrangement on a distorted Kagomé network. This is consistent with the fact that the pyrochlore lattice can be deconstructed into Kagomé layers stacked parallel to the body diagonal of the unit cell. Thus, the magnetic behavior of t-$Li_2Mn_2O_4$ is surprisingly similar to that of the topologically distinct o-$LiMnO_2$ but very different from that of the isomorphic spinels λ-MnO_2 and $LiMn_2O_4$. Both of these materials exhibit significant short-range spin−spin correlations arising from the frustrated Mn sublattice but both also order in three dimensions at 32 K (λ-MnO_2) and 65 K ($LiMn_2O_4$). The reasons for the stabilization of an apparently two-dimensional short-range order in t-$Li_2Mn_2O_4$ rather than long-range three-dimensional order, as might be expected from the topology of the Mn sublattice in $LiMn_2O_4$, are not readily apparent.

Acknowledgment. J.E.G. is supported by the Natural Sciences and Engineering Research Council of Canada, and A.S.W., currently by the TMR program of the EC. We thank Dr. Ian Swainson and Ron Donaberger for assistance with the neutron scattering experiments at the Chalk River Nuclear laboratories.

CM990175B